NMR Investigation of the Quasi-Brine Layer in Ice/Brine Mixtures

H. Cho,*,† P. B. Shepson,‡ L. A. Barrie,†,|| J. P. Cowin,† and R. Zaveri†

Pacific Northwest National Laboratory, P. O. Box 999, Richland, Washington 99352, and Departments of Chemistry, and Earth and Atmospheric Sciences, Purdue University, 1393 Brown Building, West Lafayette, Indiana 47907

Received: February 19, 2002; In Final Form: August 8, 2002

We report the study of a liquidlike phase that is found in dilute NaCl aqueous solutions frozen at temperatures below the liquid-to-solid-phase transition temperatures of H_2O and $NaCl{\cdot}2H_2O$. There is strong evidence that heterogeneous reactions of gases with halides in liquid layers on ice are the source of halogen radicals that destroy the lower tropospheric ozone, and a subeutectic brine phase is thus of particular relevance to discussions of atmospheric composition and its dependence on the chemistry of polar marine ice and snow. The fractions and concentrations of water and NaCl in this subeutectic quasi-liquid phase were measured by ^1H and ^{23}Na NMR spectroscopy, and the experimental results compared to predictions derived from an equilibrium thermodynamic analysis. The temperature dependence of the salt concentration is well-described by the equilibrium theory for temperature ranges where ideal solution behavior holds; for lower temperatures, where the observed salt concentration increases and deviations from ideality emerge, the predicted concentrations are generally higher than experimental measurements.

1. Introduction

The phase diagrams of aqueous salt solutions typically indicate that as the temperature of the liquid is decreased below the (depressed) freezing point, pure ice will be the first solid to precipitate. It follows that the surfaces and boundaries of the ice will be dominated by increasingly salt-rich phases with chemical and physical properties that differ significantly from the pure ice substrate.

The implications of this picture for the chemistry of polar aerosols and ice in the polar marine boundary layer have been the subject of extensive investigation. Recent work in this area has been motivated by the finding that periods of reduced ozone levels in the Arctic marine boundary layer are correlated with the presence of halogen species in the boundary layer.[1] Several groups have reported results suggesting that a substantial fraction of ozone removal is attributable to heterogeneous reactions involving halogenated species formed from surface snowpack.[2−4] Salt separation during seawater freezing is a relevant question in the proposal by Rankin et al.[5] that gas-phase halogens found in the Antarctic troposphere may be derived from oxidation of halides present on NaCl-rich "frost flowers". Recent measurements conducted at Alert, Nunavut, Canada, indicate that the halogen atom precursors Br_2 and BrCl can be produced within the snowpack.[6] As discussed by Michalowski et al.,[7] model simulations of Arctic chemistry assume the existence of a liquid layer on the surface of the snow grains where gases can dissolve and reactions take place that release reactive halogens.[8] In this model, the amount of halogen released is found to be quite sensitive to the volume of the liquid component.

In one of the first *quantitative* spectroscopic investigations of sea ice, Richardson and Keller[9,10] demonstrated that the chemically important surface brine layer of bulk sea ice could be selectively probed by nuclear magnetic resonance (NMR) spectroscopy. In particular, they showed that ^1H NMR measurements could be used to determine the fractions of water in the solid and liquid phase. A more detailed NMR study of frozen brines using modern Fourier transform methods was later reported by Mel'nichenko et al.,[11] and images of the macroscopic spatial distributions of the liquid in saltwater ice have also been obtained by NMR techniques.[12,13] In these experiments, all forms of nonsolid water were detected, including water in grain boundaries, on surfaces, and in included pores.

These past studies have focused exclusively on observation of the ^1H NMR signal, but it is clear that valuable information on the amounts and compositions of the surface brines can be obtained by examining the NMR spectra of the dissolved species as well. Most salts of interest in marine environments contain isotopes with favorable solution-state NMR properties, including ^{23}Na, ^{35}Cl, ^{14}N, ^{15}N, ^{79}Br, ^{81}Br, and others, making it possible to quantify the partitioning of salts between the solid and solution phase in ice−brine equilibria by direct observation of the dissolved cations and anions. NaBr, for example, has been found to concentrate at the ice surface when sea salt precipitates from sea salt solutions;[14] this in turn influences the amount of the disordered water. A method that could quantitatively probe the behavior of the ionic components would help answer important questions concerning the chemical reactions that can occur at the crystal surface, as well as provide useful data for examining the relationship between surface solute concentration and liquid content. A discussion of this approach and of some of the factors that make NMR spectroscopy attractive for selectively analyzing the liquid fraction of frozen brines has been given by Derbyshire.[15]

In this paper, we present the results of high-resolution NMR experiments in which ^1H and ^{23}Na are quantified in frozen saltwater solutions with a range of NaCl concentrations, and over the environmentally relevant temperature range 246−273

* To whom correspondence should be addressed. E-mail: hm.cho@pnl.gov.
† Pacific Northwest National Laboratory.
‡ Purdue University.
|| Present address: Atmospheric Research and Environment Programme, World Meteorological Organization, 7 bis, avenue de la Paix, CH-1211 Geneva 2, Switzerland.

10.1021/jp020449+ CCC: $22.00
Published on Web 10/08/2002

K. The results are used to develop relationships that make it possible to predict the liquid water fractions as a function of ionic strength and temperature and are applied to the study of frozen seawater.

2. Experimental Section

2.1. NMR Spectroscopy. NMR spectra were recorded using a Chemagnetics CMX Infinity console equipped with a 5 mm HX liquids probe (Nalorac Corp.). Both ^{1}H and ^{23}Na chemical shifts were referenced with 25 mM 3-(trimethylsilyl)-1-propanesulfonic acid sodium salt (DSS) (Sigma) dissolved in 99.9% $^{2}H_2O$. The lack of an adequate lock signal in experiments with frozen samples made it necessary to freeze the Z0 shim after frequency-referencing, and operate the spectrometer with the field lock apparatus disabled. The field drift for the 7.04 T magnet (Oxford Instruments, Inc.) used in this work was measured and found to be negligible (<0.05 ppm/day) for the results presented here.

The probe tuning and pulse widths were monitored over a range of temperatures and salt concentrations to ensure the comparability of signal intensities under different experimental conditions. The temperature sensor of the NMR probe was calibrated from 213 to 298 K with the proton spectrum of a methanol standard.[16] The variation in temperature over the detected region of the sample was estimated to be <0.3 K on the basis of measurements with methanol and pure water samples. The source of the dry cooling gas for low-temperature experiments was a pressurized liquid nitrogen dewar. For sample volumes >100 μL, 5 mm NMR tubes with a 0.77 mm wall thickness (Wilmad) were used to prevent tube breakage upon freezing; regular (thin-wall) NMR tubes were used for liquid volumes ≤100 μL. The tubes were filled under atmospheric conditions and sealed with a standard NMR tube cap.

Samples consisted of NaCl(aq) solutions prepared in the 1.1×10^{-3} to 0.5 M range and one seawater sample. In all experiments, the ice was formed in the NMR tube by rapidly dropping the temperature of the sample when in the NMR probe to the lowest experiment temperature, followed by a 10 min minimum equilibration period. The sample temperature was decreased from ambient to 228 K typically in about 15 min. The sample temperature was then raised through the series of experimental temperatures, with a >5 min hold time before initiation of the NMR scans. The heating of the sample was slowed as the set points were approached to prevent temperature overshoot. The ^{1}H and ^{23}Na spectra were acquired sequentially at each temperature with the decoupling and broadband channels of the same probe, respectively.

The two liquid-to-solid-phase transitions of supercooled H_2O and $NaCl{\cdot}2H_2O$ in dilute NaCl solutions (<16 wt % NaCl) have been observed to occur at temperatures between 260 and 240 K.[17,18] In all experiments reported here, the samples were cooled to 228 K before the start of the NMR measurements. The progress of freezing could be followed at short intervals by rapidly scanning the liquid water ^{1}H NMR line and monitoring its disappearance as the temperature dropped below phase transition points. Most solutions in the present study were found not to begin solidifying until the temperature was reduced below 257 K. Once freezing began, the process was rapid, with the largest changes in the NMR signal complete within a few seconds. At temperatures above the first liquid-to-solid transition temperature, the water ^{1}H resonance can be used as a temperature indicator to verify that the solution is supercooling. The observed temperature dependence of the ^{1}H shift of a pure water sample measured at 299.98 MHz is displayed in Figure 1. As shown in this figure, water chemical shifts at presumptive temperatures below the freezing point obey the same temperature dependence as shifts measured at temperatures above 0 °C, which implies that the solution is indeed being supercooled to temperatures well below the freezing point. A detailed study of the temperature dependence of liquid and gaseous water has been reported by Hindman,[19] whose results are quantitatively consistent with the data in Figure 1.

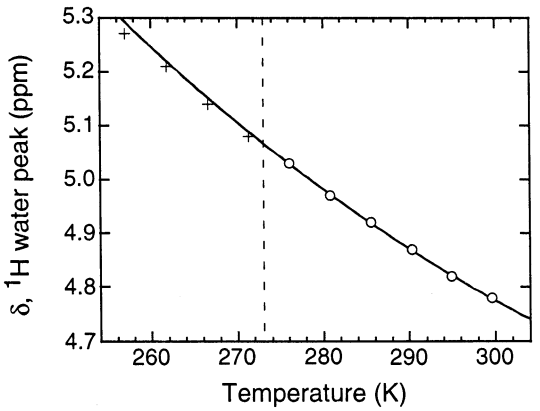

Figure 1. Temperature dependence of the ^{1}H chemical shift of a pure water sample. Observed full-width half-height line widths are less than the widths of the markers. The line is a least-squares fit of data measured at temperatures above 273.15 K (circles) to the equation $\alpha T^2 + \beta T + \gamma$, with $\alpha = 7.315 \times 10^{-5}$, $\beta = -5.276 \times 10^{-2}$, and $\gamma = 14.021$. Shifts measured at temperatures below 273.15 K are symbolized as crosses; no ice had formed at these temperatures.

2.2. Sample Preparation. NaCl (Aldrich, 98+%), was used as received, and diluted in deionized, carbon-filter purified water (18.0 MΩ cm). All solutions were likely saturated with dissolved gases from the ambient air (with its trace CO_2). The presence of dissolved gases potentially introduces complications in the interpretation of the results but is a more realistic representation of the conditions in oceanic systems. The seawater sample was collected from the ocean surface at the Strait of Juan de Fuca in Washington State in December 2000 and used without treatment or filtration.

3. Results

The ^{1}H NMR signals of water and ice are readily differentiated on the basis of line width; although they overlap, the water resonance has a width that can be more than 4 orders of magnitude narrower than the line width for polycrystalline ice, which is of the order of 10^5 Hz.[20] Similarly, the ^{23}Na resonance line width for Na^+ in aqueous solution can be more than a factor of 100 narrower than the resonance of NaCl(s) (ca. 3 kHz) or $NaCl{\cdot}2H_2O$. ^{1}H (Figure 2) and ^{23}Na (Figure 3) NMR spectra of frozen $NaCl/H_2O$ solutions were found to exhibit resonances that, although broader and weaker than unfrozen room temperature solutions, were nonetheless considerably narrower than the lines from expected solid phases. In addition to the line widths, the ^{23}Na resonances for the frozen solutions were found to have nutation frequencies and short relaxation times more characteristic of sodium species in a solution, rather than solid, phase.[21,22] We thus interpret the integrated ^{1}H resonance for these frozen solutions as representative of water in a liquid state, associated with the NaCl brine.

The relative amounts of ^{1}H and ^{23}Na contained in this phase can be determined at every temperature from the rigorous proportionality of the nuclide concentration to the integrated intensity of the NMR line. Complications with this method can arise if a detectable fraction of the ^{23}Na signal originates from

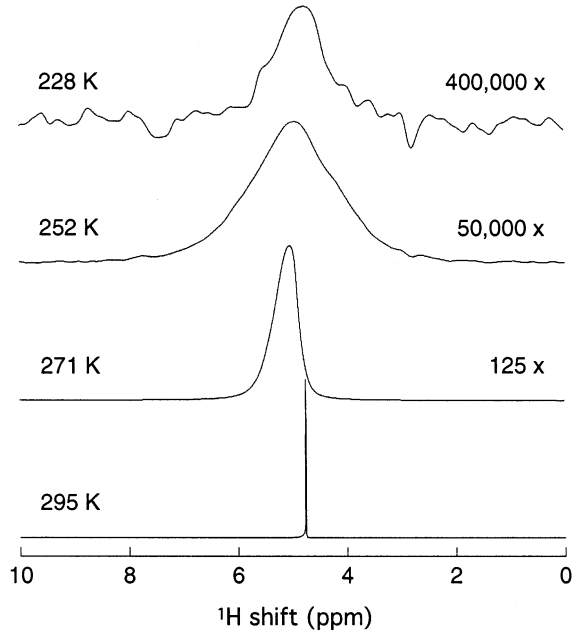

Figure 2. ^{1}H NMR spectra of a brine solution ([NaCl] = 0.500 M) at different temperatures. Relative intensity scales are given by the factors on the right. Each spectrum is an average of four scans. The time domain signals were apodized, but in no case was the width of the apodization function more than 20% of the intrinsic width of the ^{1}H line.

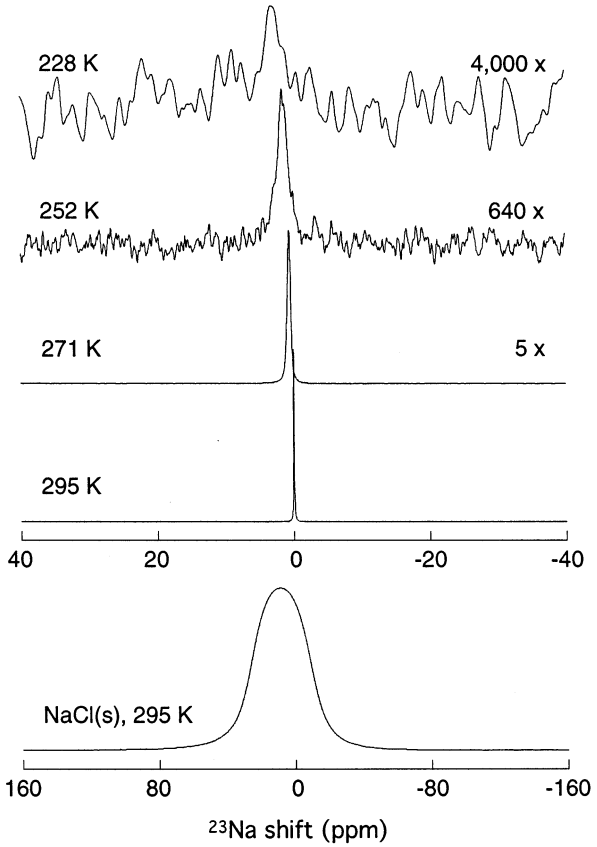

Figure 3. ^{23}Na NMR spectra for the same sample and temperatures as in Figure 2, along with a spectrum of pure NaCl(s) (bottom, with expanded chemical shift axis). Vertical scaling is on the right. Each brine spectrum is an average of 256 scans. As for Figure 2, the width of the apodization function was ≤20% of the width of the actual resonance.

sodium atoms in a noncubic solid,[22] but the line width, nutation, and relaxation data suggest that this was not the case with the

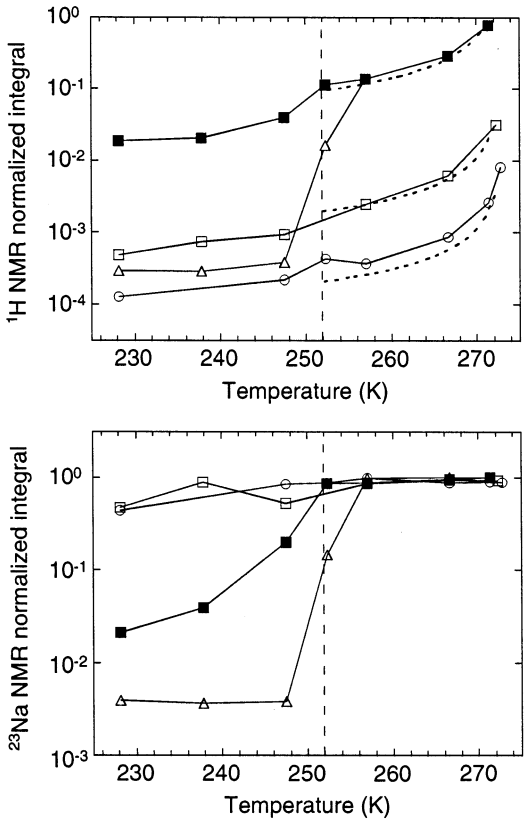

Figure 4. Plot of the integral of the detected fraction of the ^{1}H (top) and ^{23}Na (bottom) NMR signals as a function of sample temperature. The integrals have been normalized to the integrals of signals detected at 294.9 K. Three NaCl concentrations are represented: 0.0011 M (circles), 0.0104 M (squares), and 0.500 M (triangles). Seawater data are shown in black squares. The eutectic temperature is indicated by the dashed vertical line. The short dashed lines represent the calculated liquid water fraction based on freezing point depression. The lines connecting data points are guides for the eye.

frozen solutions investigated in this study. The results of this determination for three different NaCl concentrations (0.0011, 0.0104, and 0.5 M) are shown in Figure 4. A pure water sample was examined in the same way, but the intensity of the liquid fraction signal was small compared to the brine samples, even for temperatures approaching 273.15 K, and the data have not been plotted. In Figure 4, the integrated intensities used to compute the liquid fractions have been normalized to the integrals measured at 295 K and adjusted for the Curie Law ($1/T$) dependence of the nuclear magnetization on temperature.[23] The data for a seawater sample (for which $[Na^{+}] = 0.46$ M) are also shown; the high liquid fraction for this sample below the eutectic point is presumably due to the presence of other salts that have a lower eutectic than NaCl (in particular, $MgSO_4$ and $MgCl_2$). We note from the bottom panel of Figure 4 that for the 0.5 M sample more than 99% of the NaCl precipitates as $NaCl{\cdot}2H_2O$ at the eutectic point, but for the more dilute samples typically more than half of the initial Na^{+} remains in a free ionic state to as low as 228 K. We interpret this as a kinetic effect of the competing rates of diffusion of the ions prior to precipitation, and solidification of the pure ice phase.

A simple model for computing the liquid fraction above the eutectic temperature can be developed from the phase diagram of NaCl−water mixtures. The phase diagram[18] suggests that as the frozen solid is warmed above the eutectic temperature, the brine formed upon melting will have a temperature-dependent NaCl concentration. The expected NaCl concentration of a brine in equilibrium with ice for temperatures 252 K < T < 273.15

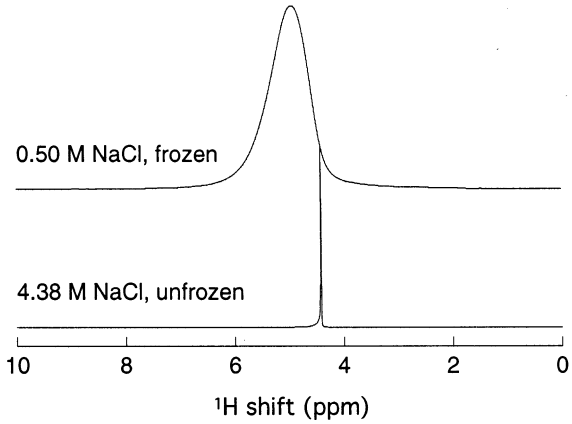

Figure 5. ^{1}H spectra for a frozen 0.5 M NaCl sample at 257 K, and a supercooled 4.38 M NaCl solution.

K can be estimated from the positive root of the quadratic equation $0 = ax^2 + bx + T - 273.15$, which is the least-squares fit of a second-order polynomial to published freezing point depression data of NaCl(aq),[24] with $a = 0.167$ and $b = 3.137$. The meaningful solution of this equation, which gives the NaCl concentration at temperature T, will be written as $x = [\mathrm{NaCl}]_{\mathrm{FPD},T}$. If we assume that all of the NaCl enters the solution phase as the solid is warmed above the eutectic temperature, then the freezing point depression model implies that the liquid fraction $\phi_{\mathrm{H_2O}}(T)$ is given by eq 1, where the numerator is the concentration in the completely melted sample:

$$\phi_{\mathrm{H_2O}}(T) = [\mathrm{NaCl}]_0/[\mathrm{NaCl}]_{\mathrm{FPD},T} \qquad (1)$$

Curves computed with this model are shown as the dotted lines in Figure 4 (top), for each initial sample concentration. As shown in Figure 4, the theory matches well with the measurements but systematically underestimates the liquid fraction. The above model treats the liquid fraction as a concentrated brine with a depressed freezing point, in equilibrium with pure ice. The concentration of this hypothetical brine can be computed as $[\mathrm{NaCl}]_{\mathrm{FPD},T}$, and therefore a direct comparison can be made with the brine in this brine/ice mixture and a brine prepared at room temperature with the same concentration and cooled to the temperature T. One such comparison is illustrated in Figure 5, which shows the ^{1}H spectrum for 0.5 M NaCl sample frozen at 228 K and warmed to 257 K (i.e., unfrozen), along with the spectrum of a 4.38 M NaCl solution prepared at room temperature and cooled to 257 K. The latter concentration is close to that required for a 16 K freezing point depression, i.e., it is the NaCl concentration on the surface of the frozen 0.5 M NaCl sample, if this model applies. As shown in Figure 5, the peak width for the frozen 0.5 M sample is much broader than for the brine sample.

A significant amount of liquidlike water is present below the temperature (the NaCl·2H$_2$O eutectic point) at which all NaCl should have precipitated as sodium chloride dihydrate (Figure 4). This is observed for temperatures as much as ~23 K below the eutectic point. This will be discussed below.

4. Discussion

According to an idealized interpretation of the Gibbs phase rule[25,26] and the phase diagram of NaCl and water,[18] NaCl(aq) solutions solidify completely at temperatures below the eutectic point (~252 K) to a mixture of pure ice, NaCl(s), and NaCl·2H$_2$O(s), for all initial salt concentrations. The finding that a liquid brine phase can coexist with large amounts of ice and solid sodium salts at temperatures more than 20 K below the eutectic point, as exemplified by the data in Figure 4, would therefore represent an apparent deviation from ideal equilibrium behavior. To differentiate this unfrozen brine phase from the "quasi-liquid layer" (QLL) previously found in studies of bulk pure water ice,[27−35] we refer to the solution phase as a "quasi-brine layer", or QBL.

The coexistence of a liquid brine phase with pure ice at temperatures below the eutectic point is indicated in experiments reported by Thurmond and Brass[17] and Koop et al.[18] Using differential scanning calorimetry (DSC), Koop et al. observed two separate thermal emission events during cooling of dilute NaCl solutions, which they attributed to the supercooled-liquid-to-solid-phase transitions associated with (1) the formation of pure ice and (2) the precipitation of NaCl·2H$_2$O. The temperatures of these two phase transitions converge as the NaCl concentration increases and become essentially equal for concentrations above 16 wt % NaCl. For all [NaCl] values investigated by them, the second of these phase transitions occurred at temperatures below the eutectic point, the latter having been determined by warming the completely solidified mixture. Flow cell microscopy measurements of the deliquescence and efflorescence points of NaCl(aq) droplets by Koop et al., provided additional evidence of a nonsolid intermediate brine phase, which they have called a metastable liquid.

Despite the superficial resemblance, the supercooled brine/ice mixture found in the DSC experiments differs in at least two important respects from the QBL observed in the present study. The DSC experiments showed that as the temperature was reduced below 240 K, NaCl·2H$_2$O precipitated over a narrow temperature range. The QBL phase observed in the NMR experiments, on the other hand, was seen in samples cooled to temperatures >20 K below the supercooled-liquid-to-solid transition temperature of NaCl·2H$_2$O. In other words, the QBL is found below the temperature range where supercooled brine/ice mixtures are presumed to exist on the basis of the DSC work.

A second difference is found when the samples are warmed from the lowest temperature to the NaCl·2H$_2$O liquid-to-solid transition. The thermograms recorded in the DSC work reveal the first well-defined endotherm at the eutectic temperature, suggesting that no melting occurs until around 252 K. This contrasts with the behavior of the QBL fraction, which grows as the sample is warmed from 228 K, as shown in Figure 4. For example, in both the 0.001 and 0.01 M NaCl solutions the QBL fraction approximately doubled as the samples were warmed from 228 to 247 K.

To emphasize that the subeutectic brine/ice mixtures observed in the DSC work differs in certain characteristics from the QBL observed in the NMR experiments, we will refer to the supercooled brine seen below the first liquid-to-solid-phase transition (i.e., water → ice) in the DSC experiments by the separate name metastable brine layer, or MBL. The interpretation of the events during one cooling/warming cycle, as implied by the DSC and NMR experiments, is portrayed in Figure 6. Because the liquid can be supercooled, the state of the system does not follow the same path during cooling and warming, resulting in a hysteresis effect.

The MBL observed in the DSC experiments presents no inconsistencies vis-à-vis the Gibbs phase rule and the water/NaCl phase diagram, because these concepts are valid only for systems at thermodynamic equilibrium. As a metastable state, the MBL cannot be described as an equilibrium system. It is less clear, however, how to represent the QBL detected in the NMR experiments. In particular, one must ask if the samples

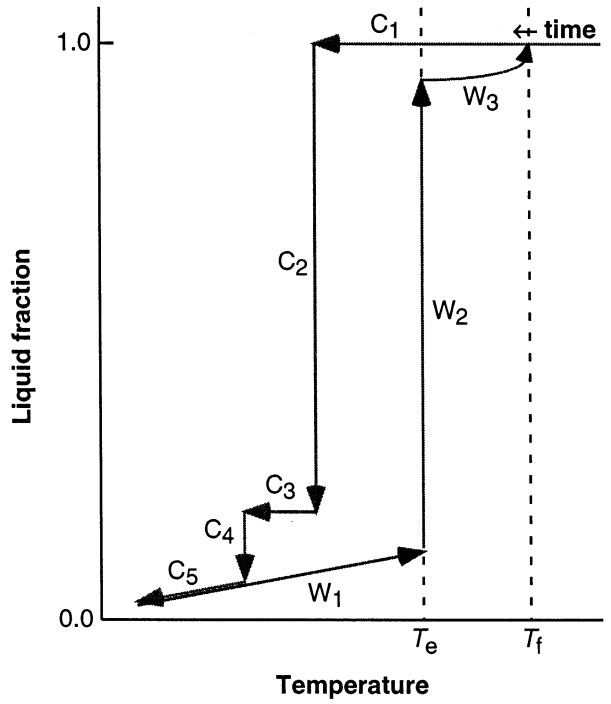

Figure 6. Evolution of the liquid fraction during a cooling and warming cycle of a NaCl solution, as suggested by DSC and NMR experiments. Time proceeds in the direction indicated by the arrows; the freezing temperature (T_f) and the eutectic temperature (T_e) are shown by the dashed vertical lines. When the liquid brine is first cooled (C_1), no phase transition is observed, and thus the liquid is metastable below T_f. During C_2, pure ice suddenly precipitates, evolving heat, and the liquid fraction drops, but not to zero. The remaining MBL is cooled during C_3 until a second phase transition occurs (C_4), resulting in a second exothermal event and a drop in the liquid fraction. A liquid phase, the QBL, nonetheless remains, as revealed by the NMR experiments, and can be cooled during C_5. Upon warming (W_1), the liquid fraction gradually increases until T_e is reached, whereupon rapid melting begins and the liquid fraction jumps. This sudden melting stops when the resulting brine reaches the approximate concentration dictated by the freezing point depression curve, and the liquid fraction rises smoothly thereafter as the temperature is raised (W_3) and melting continues.

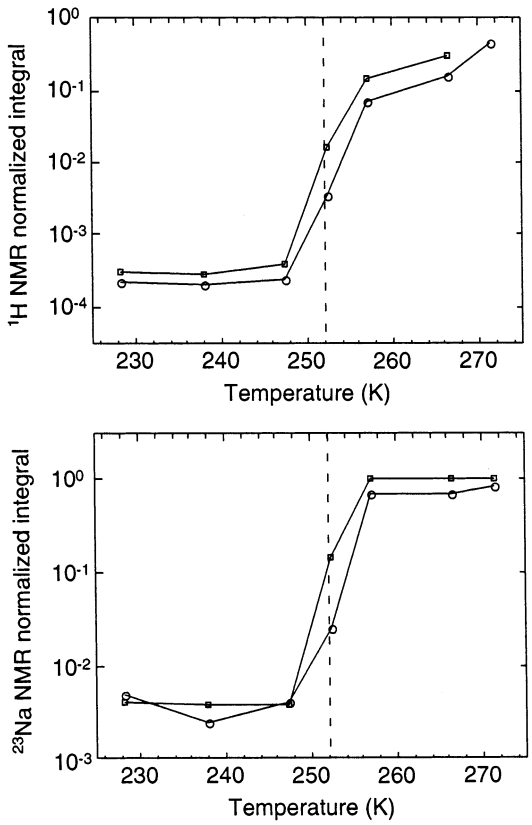

Figure 7. Comparison of integrated ^{1}H (top) and ^{23}Na (bottom) NMR signals for short (squares) and long (circles) samples, with [NaCl] = 0.500 M. The integrals are normalized as in Figure 4.

had achieved full thermodynamic equilibrium at every temperature, or if slower freezing and a more protracted annealing period might be required to guarantee equilibration. Koop et al.[18] have presented evidence indicating that a supercooled brine can undergo rapid heterogeneous nucleation on pure ice surfaces once the temperature is reduced to a certain threshold (~240 K for low [NaCl]). Presumably, if the QBL were a metastable state, it too would be susceptible to solidification and short equilibration times below the threshold nucleation temperature. The monotonic growth of the QBL fraction as the samples were warmed from 228 K to the eutectic temperature is suggestive of a reversible melting process, which would also be inconsistent with the characterization of the QBL as a nonequilibrium state. Recent work on the theory of ice premelting[35−37] explains the presence of liquid water at these temperatures not as a metastable condition, but as an equilibrium between solid−vapor, solid−solid, and solid−wall interfaces.

In addition to the assumption of thermodynamic equilibrium, the Gibbs phase rule and the phase diagram of a water/NaCl mixture apply to ideal systems at constant pressure and under conditions that exclude all other phases and components, including air and other gases. These conditions were not realized in the NMR experiments in which the water/NaCl mixtures were in contact with air under uncontrolled pressures in a sealed NMR tube. Moreover, no special measures were taken to degas the samples prior to cooling. These factors represent minor deviations from an idealized experiment, and any modification of the phase diagram may also be expected to be manifested in small deviations from ideal behavior.

The spatial distribution of the QBL, Na^+, and Cl^- in the samples cannot be determined from the information obtained in these experiments. However, these methods do provide a way to investigate one hypothetical distribution, namely, the distribution resulting from a migration of the salt ions to the top (or bottom) surfaces of the sample upon freezing. The liquid column of the samples investigated in this study (i.e., for the data in Figure 4) was short enough to be entirely contained in the NMR probe's rf coil (liquid volume = 100 μL). To determine if the brine resides on the top of the ice, samples more than twice as long as the coil were prepared (liquid volume = 400 μL in a thick-wall NMR tube), so that the top and bottom volumes of the sample could be positioned outside the coil's sensitive volume. Results comparing the signals for 100 and 400 μL samples (for 0.5 M NaCl) are shown in Figure 7. At a concentration of 0.5 M, the fraction of the water in the QBL phase was typically greater for the short sample than for the long sample. The ratio $(^1\text{H signal})_{100}/(^1\text{H signal})_{400}$ was 1.38 at T = 228.1 K, increased to 4.64 near the eutectic point (T = 252.3 K), and then decreased to 1.93 as the temperature increased to 266.6 K. For the 1.1×10^{-3} M samples (not shown in Figure 7) this ratio displays less variability, fluctuating around 1.36(±0.16) at temperatures above the eutectic point. These data suggest that there is some preferential migration of the QBL outside the central region of the sample as freezing occurs.

The equations of equilibrium thermodynamics provide a way to derive a predicted [NaCl] dependence on temperature for direct comparison with the experimental results. According to

standard thermodynamic treatments, the solvent mole fraction of an ideal solution at equilibrium is given by the relation[26,38]

$$\ln x_{H_2O}(T) = -\frac{\Delta H_f^0}{R}\left(\frac{1}{T} - \frac{1}{T_f}\right) \quad (2)$$

where ΔH_f^0 is the enthalpy of fusion, R is the ideal gas constant, T_f is the freezing temperature of the pure solvent, and $x_{H_2O}(T)$ is the mole fraction of the solvent H_2O in the liquid phase, defined as

$$x_{H_2O}(T) \equiv \frac{N_{H_2O}(T)}{N_{H_2O}(T) + \sum_{j=1}^{P} N_j(T)} \quad (3)$$

The quantity $N_{H_2O}(T)$ is the number of moles of liquid solvent (water) at temperature T, and the summation in the denominator is over the P solutes in solution.

If we assume that the solute concentration is low, so $N_{H_2O}(T) \gg \sum_{j=1}^{P} N_j(T)$, then eq 2 can be simplified to

$$\frac{\sum_{j=1}^{P} N_j(T)}{N_{H_2O}(T)} \approx \frac{\Delta H_f^0}{R}\left(\frac{1}{T} - \frac{1}{T_f}\right) \quad (4)$$

This equation can be modified to

$$\frac{\sum_{j=1}^{P} \bar{c}_j \phi_j(T)}{\phi_{H_2O}(T)} \approx \frac{1000 \Delta H_f^0}{\bar{m}_{H_2O} R T_f}\left(\frac{T_f - T}{T}\right) \quad (5)$$

Here $\phi_{H_2O}(T)$ and $\phi_j(T)$ represent the fractions of solvent and solute, respectively, that are in the liquid phase, $\bar{m}_{H_2O}$ is the molecular weight of water, and $\bar{c}_j$ is the molal concentration of the jth solute of the completely unfrozen solution. Note that $\bar{c}_j\phi_j(T)/\phi_{H_2O}(T)$ is simply the molal concentration of the jth solute in the liquid phase at temperature $T < T_f$, which means that

$$\frac{\sum_{j=1}^{P} \bar{c}_j \phi_j(T)}{\phi_{H_2O}(T)} = \text{sum of all solute concentrations in QBL at temperature } T$$

$$= C_T(T) \quad (6)$$

Substituting this expression into eq 5, we find

$$C_T(T) \approx \frac{1000 \Delta H_f^0}{\bar{m}_{H_2O} R T_f}\left(\frac{T_f - T}{T}\right) \quad (7)$$

This relation predicts that a plot of $C_T(T)$ vs $(T_f - T)/T$ will be a straight line with slope and y-intercept equal to $1000\Delta H_f^0/\bar{m}_{H_2O}RT_f$ and zero, respectively. The theoretical prediction and experimental results are compared in Figure 8 for all data, including those of the seawater sample. The concentrations of Na^+ and Cl^- were determined from the NMR integrals; for other solutes (present in the seawater), it was assumed that $\phi_j(T) = 1$ at all temperatures in the computation of $C_T(T)$. The ion concentrations of the seawater at room temperature were assumed to be $[Cl^-] = 0.535$ M, $[Na^+] = 0.459$ M, $[SO_4^{2-}] = 0.0276$ M, $[Mg^{2+}] = 0.0523$ M, $[Ca^{2+}] = 0.0100$ M, and $[K^+] = 0.0097$ M. The points corresponding to the seawater measurement are systematically higher than the theoretical prediction, suggesting that the agreement of theory and experiment would be improved if it was assumed other solutes had precipitated, giving $\phi_j(T) < 1$ for some of the other ions.

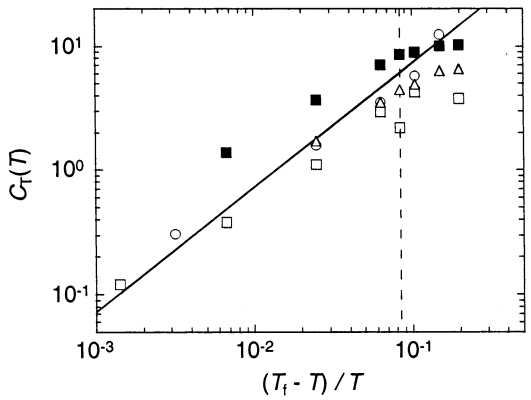

Figure 8. Log−log plot of the total molal solute concentration in the liquid phase vs $(T_f - T)/T$. Data symbols are the same as for Figure 4. The dashed vertical line indicates the position of the eutectic temperature, and the solid line represents the theoretically predicted behavior (eq 7).

The increase in the absolute deviation and scatter of the experimental points for increasing $(T_f - T)/T$ is mainly a product of two factors. First, the ^{23}Na and ^1H NMR signals rapidly become smaller as T decreases (see Figures 2 and 3), which means that the experimental uncertainty in determining $C_T(T)$ grows with increasing $(T_f - T)/T$. The second factor involves the approximation of substituting concentrations for activities in the derivation of eq 7. As T decreases and the solute concentrations in the liquid-phase become greater, the deviations in the experimental observations from ideal behavior can be expected to become more pronounced. Nonetheless, it is notable that there is not a large departure from the theoretical slope for temperatures below the eutectic point for $NaCl{\cdot}2H_2O$ (i.e., to the right of the dashed line), given the equilibrium model assumed in the theory.

According to eq 7, the fraction of H_2O in the QBL has an upper limit, which is obtained when all of the solutes are in the QBL and $\phi_j(T) = 1$ for all j. This maximum is therefore given by the expression

$$\phi_{H_2O}^{max}(T) \approx \frac{\bar{m}_{H_2O} R T_f}{1000 \Delta H_f^0}\left(\frac{T}{T - T_f}\right) C_T^0 \quad (8)$$

where $C_T^0 = \sum_{j=1}^{P} \bar{c}_j$ is the total solute concentration in the completely unfrozen brine.

Halogen activation chemistry in the Arctic depends on several key parameters, as identified by Michalowski et al.,[7] that can be estimated with eqs 7 and 8. In particular, numerical bounds can be placed on the size of the chemically reactive QBL reservoir, its pH, and the concentrations of reagents in the reservoir. Ion chromatographic analyses of snow samples from the frozen Arctic Ocean surface (where halogen activation is believed to occur[6]) on February 17, 2000 (in the dark), during the Polar Sunrise Experiment 2000 indicated a total anion content of 7.7×10^{-5} M, 89% of which was Cl^-, with the rest nearly equally distributed between NO_3^- and SO_4^{2-}. Thus, the cation content will be mostly Na^+, with a small fraction in the form of H^+ (derived from H_2SO_4 and HNO_3). For a typical Arctic surface temperature in February of 233 K and a Na/Cl ratio in the snow that is the same as for ocean water, i.e., 0.86, we find from eq 8 that $\phi_{H_2O}^{max}(T)$ will be approximately 6.3×10^{-6}. If we assume that the anionic charge of the Cl^-, NO_3^-, and SO_4^{2-} in the QBL is balanced by only Na^+ and H^+, then the H^+ concentration can be computed to be 3.6 M.

The pH directly affects one of the key reactions believed to result in halogen activation:

$$HOBr + Cl^- + H^+ \rightleftharpoons BrCl + H_2O$$

The complex composition of real snow is likely to make its surface a high ionic strength solution, including a variety of organic species such as HCHO.

Numbers obtained with the use of eq 8 correspond to the case where all of the solute is found in the QBL and none has precipitated. The data in Figure 4 suggest that the fraction of solute in the QBL appears to be inversely related to the starting concentration of the brine, and thus we expect that eq 8 will be of greatest value for calculations involving solutions with low concentrations. The solute concentration in snow from the Arctic appears to fall into this useful low range.

5. Conclusion

The results of this study imply that highly concentrated liquid brines, which we call QBLs, can coexist with ice and solid $NaCl\cdot 2H_2O$ at temperatures as low as 228 K. In parallel experiments with a pure water sample, a far smaller liquid fraction was measured, suggesting that the added NaCl, and not dissolved gases or impurities, was the primary determinant of the volume of this liquid phase.

The QBL was observed at temperatures lower than the two first order phase transition temperatures detected in brine by DSC measurements. The liquid fraction was found to increase gradually with the temperature, and the temperature dependence of the salt concentration appears to be well described by a thermodynamic treatment that assumes a state of chemical equilibrium. Further work that systematically examines such factors as the rates of freezing and the dependence on the lowest temperature set point is required to develop a predictive description for the liquid fraction, $\phi_{H_2O}(T)$.

Because the QBL is a more reactive reservoir than ice or solid $NaCl\cdot 2H_2O$, its existence has important implications for atmospheric chemistry in Arctic environments. It is common to find surface snowpack in frozen marine areas with bulk sea salt concentrations ranging from 0.5 to 2.0 μM, e.g., in the Arctic Ocean, the edges of the Antarctic continent, and Hudson Bay. This snowpack is porous and ventilated by wind-driven air containing reactive gases that can interact with the liquid or solid surface of the snow. Gas reactions with concentrated brine layers on the outside of snow grains produce more reactive gaseous halogenated species than those generated by gas interactions with pure ice. The volume and concentration of liquid brine in the snowpack are thus key parameters of air−surface exchange in polar regions, interfacial reactions in atmospheric chemistry, and the transfer of chemicals from the atmosphere to glacial ice cores.

Acknowledgment. The Pacific Northwest National Laboratory is operated for the U.S. Department of Energy by the Battelle Memorial Institute under contract DE-AC06-76RLO-1830. P.B.S. gratefully acknowledges the support received from PNNL in conducting this work. We thank Dr. Eric Crecelius of the PNNL Marine Sciences Laboratory for the Strait of Juan de Fuca seawater sample.

References and Notes

(1) Barrie, L. A.; Bottenheim, J. W.; Schnell, R. C.; Crutzen, P. J.; Rasmussen, R. A. *Nature* **1988**, *334*, 138.

(2) Tang, T.; McConnell, J. C. *Geophys. Res. Lett.* **1996**, *23*, 2633.

(3) Impey, G. A.; Shepson, P. B.; Hastie, D. R.; Barrie, L. A.; Anlauf, K. G. *J. Geophys. Res.* **1997**, *102*, 16005.

(4) Impey, G. A.; Mihele, C. M.; Shepson, P. B.; Hastie, D. R.; Anlauf, K. G.; Barrie, L. A. *J. Atmos. Chem.* **1999**, *34*, 21.

(5) Rankin, A. M.; Auld, V.; Wolff, E. W. *Geophys. Res. Lett.* **2000**, *27*, 3469.

(6) Foster, K.; Plastridge, R.; Bottenheim, J.; Shepson, P.; Finlayson-Pitts, B.; Spicer, C. W. *Science* **2001**, *291*, 471.

(7) Michalowski, B.; Francisco, J. S.; Li, Y.; Li, S.-M.; Shepson, P. B. *J. Geophys. Res.* **2000**, *105*, 15131.

(8) Conklin, M. H.; Bales, R. C. *J. Geophys. Res.* **1993**, *98*, 16851.

(9) Richardson, C.; Keller, E. E. *J. Glaciology* **1966**, *6*, 89.

(10) Richardson, C. *J. Glaciology* **1976**, *17*, 507.

(11) Mel'nichenko, N. A.; Mikhaylov, V. I.; Chizhik, V. I. *Okeanologiya* **1979**, *19*, 811.

(12) Edelstein, W. A.; Schulson, E. M. *J. Glaciology* **1991**, *37*, 177.

(13) Menzel, M. I.; Han, S.-I.; Stapf, S.; Blümich, B. *J. Magn. Reson.* **2000**, *143*, 376.

(14) Zangmeister, C. D.; Turner, J. A.; Pemberton, J. E. *Geophys. Res. Lett.* **2001**, *28*, 995.

(15) Derbyshire, W. The Dynamics of Water in Heterogeneous Systems. In *Water: A Comprehensive Treatise*; Franks, F., Ed.; Plenum Press: New York, 1982.

(16) Van Geet, A. L. *Anal. Chem.* **1970**, *42*, 679.

(17) Thurmond, V. L.; Brass, G. W. Geochemistry of freezing brines: Low-temperature properties of sodium chloride. CRREL Report 87-13; U.S. Army Cold Regions Research and Engineering Laboratory: Hanover, NH, 1987.

(18) Koop, T.; Kapilashrami, A.; Molina, L. T.; Molina, M. J. *J. Geophys. Res.* **2000**, *105*, 26393.

(19) Hindman, J. C. *J. Chem. Phys.* **1966**, *44*, 4582.

(20) Barnaal, D. E.; Lowe, I. J. *J. Chem. Phys.* **1966**, *46*, 4800.

(21) Akitt, J. W. The Alkali and Alkaline Earth Metals: Lithium, Sodium, Potassium, Rubidium, Cesium, Beryllium, Magnesium, Calcium, Strontium, and Barium. In *Multinuclear NMR*; Mason, J., Ed.; Plenum Press: New York, 1987.

(22) Freude, D.; Haase, J. Quadrupolar Effects in Solid-State Nuclear Magnetic Resonance. In *NMR Basic Principles and Progress*; Diehl, P., Fluck, E., Günther, H. Kosfeld, R., Seelig, J., Eds.; Springer-Verlag: Berlin, 1993; Vol. 29.

(23) Slichter, C. P. *Principles of Magnetic Resonance*, 3rd ed.; Springer-Verlag: New York, 1990.

(24) Lide, D. R., Ed. *CRC Handbook of Chemistry and Physics*, 79th ed.; CRC Press: Boca Raton, FL, 1999.

(25) Findlay, A.; Campbell, A. N.; Smith, N. O. *The Phase Rule and Its Applications*, 9th ed.; Dover Publications: New York, 1951.

(26) Gokcen, N. A. *Thermodynamics*; Techscience Inc.: Hawthorne, CA, 1975.

(27) Akitt, J. W.; Lilley, T. H. *Chem. Commun.* **1967**, 323.

(28) Clifford, J. *Chem. Commun.* **1967**, 880.

(29) Bell, J. D.; Myatt, R. W.; Richards, R. E. *Nature (London) Phys. Sci.* **1971**, *230*, 91.

(30) Kvilidze, V. I.; Kiselev, V. F.; Kurzaev, A. B.; Ushakova, L. A. *Surf. Sci.* **1974**, *44*, 60.

(31) Nason, D.; Fletcher, N. H. *J. Chem. Phys.* **1975**, *62*, 4444.

(32) Golecki, I.; Jaccard, C. *J. Phys. C: Solid State Phys.* **1978**, *11*, 4229.

(33) Ocampo, J.; Klinger, J. *J. Phys. Chem.* **1983**, *87*, 4325.

(34) Mizuno, Y.; Hanafusa, N. *J. Physique C1* **1987**, *48*, C1−511.

(35) Sadtchenko, V.; Ewing, G. E. *J. Chem. Phys.* **2002**, *116*, 4686.

(36) Dash, J. G.; Fu, H.-Y.; Wettlaufer, J. S. *Rep. Prog. Phys.* **1995**, *58*, 115.

(37) Wettlaufer, J. S. *Phys. Rev. Lett.* **1999**, *82*, 2516.

(38) Mahan, B. H. *University Chemistry*, 3rd ed.; Addison-Wesley: Reading, MA, 1975.